

# The effect of Nd concentration on the spectroscopic and emission decay properties of highly doped Nd:YAG ceramics

V. Lupei, A. Lupei, and S. Georgescu

*Institute of Atomic Physics, Solid State Quantum Electronics Laboratory, 76900 Bucharest, Romania*

T. Taira and Y. Sato

*Laser Research Center, Institute for Molecular Science, Okazaki 444-8585, Japan*

A. Ikesue

*Japan Fine Ceramics Center, 2-4-1 Mutsuno, Atsuta-ku Nagoya 456-8587, Japan*

(Received 15 March 2001; published 15 August 2001)

High-resolution optical spectroscopy shows that no additional defects or large-scale deformations take place in Nd:YAG ceramics doped with up to 9 at. % Nd as compared to the diluted single crystals. Spectral satellites connected with ensembles of Nd ions, predicted by the statistics of a random distribution over the available lattice sites, are observed at low temperatures. At higher temperatures the resolution is lost and these ensembles contribute to an inhomogeneous broadening of the lines. At room temperature the global emission decay of  ${}^4F_{3/2}$  is nonexponential and can be explained by the common effect of a direct donor-acceptor transfer process with parameters determined earlier for diluted crystals and by a migration-assisted transfer whose ensemble-averaged rate depends quadratically on the Nd concentration  $C_{Nd}$ . The calculated quantum efficiency  $\eta$  and the figure of merit  $\eta C_{Nd}$  indicate that concentrated Nd:YAG components are suitable for continuous-wave laser emission and, coupled with resonant hot band pumping into the emitting level, they show the prospect for scaling Nd:YAG lasers to very high powers.

DOI: 10.1103/PhysRevB.64.092102

PACS number(s): 78.55.Kz, 42.70.Hj, 42.55.Rz

## I. INTRODUCTION

The renewed interest in the use of highly concentrated Nd:YAG laser materials for constructing solid-state lasers raises important questions concerning the effect of Nd concentration ( $C_{Nd}$ ) on the spectroscopic and emission decay characteristics that determine the performances of these lasers. Highly doped Nd:YAG components can be produced by various techniques such as crystal growth by the thermal gradient technique<sup>1</sup> (small- or medium-size components with up to 3–4 at. % Nd, strong variation of  $C_{Nd}$  along the growth axis) or flux<sup>2</sup> (small components of up to 4–5 at. % Nd), epitaxial thin film deposition<sup>3</sup> ( $C_{Nd}$  up to 15 at. %), or ceramic techniques<sup>4</sup> ( $C_{Nd}$  up to 9 at. %, medium or large components with uniform doping profile). The last technique has the additional advantages of simplicity, high yield, and low production costs. The high  $C_{Nd}$  in YAG raises also basic problems concerning the state of the Nd ions in a host that offers for substitution a smaller ion as well as characterization of the energy transfer processes between the Nd ions. Additional problems concern the state of Nd ions in ceramics as compared to single crystals.<sup>5</sup> Despite the fact that some of these components have been used in laser experiments, no detailed account of the effect of  $C_{Nd}$  on their spectroscopic and emission decay properties has been reported. This paper reports the results of spectroscopic and emission decay investigations of Nd:YAG ceramics with up to 9 at. % Nd.

## II. EXPERIMENTAL DETAILS

High-optical-quality transparent Nd:YAG ceramics with up to 9 at. % Nd have been produced by the technique described in Ref. 4. The high-resolution transmission spectra

were measured at temperatures between 10 and 300 K by using a high-resolution (better than  $0.3 \text{ cm}^{-1}$ ) 1-m double monochromator. For the emission decay a photon counting technique of 20-ns resolution was used and the excitation was made nonselectively at room temperature with the second harmonic of a Q-switched Nd:YAG laser (10-ns pulse width). The intensity of excitation was kept low in order to avoid a high population of the emitting level  ${}^4F_{3/2}$  (under  $\sim 1\%$ ), which could favor upconversion by excited-state absorption or energy transfer.

## III. EXPERIMENTAL RESULTS AND DISCUSSION

The transmission spectra of Nd:YAG ceramic samples of 1 at. % Nd are similar to those of single crystals<sup>5</sup> of the same  $C_{Nd}$ . No obvious line shifts or broadenings have been observed in any spectral range, in agreement with previous investigations on 1 at. % Nd:YAG ceramics.<sup>6</sup> This indicates that in these ceramics the Nd ions reside at the dodecahedral  $c$  site of  $D_2$  symmetry of the garnet lattice and no large-scale distortion of the crystalline lattice occurs as compared to single crystals. Thus the recent studies<sup>7–9</sup> on the  $D_2$  symmetry site of  $\text{Nd}^{3+}$  in YAG crystals remain valid in the case of the ceramics, too. With increasing Nd concentration the positions of the spectral lines remain practically unchanged with very slight shifts for some of the optical transitions and with a selective broadening.

The structures of the satellites in the low-temperature high-resolution spectra at 1 at. % Nd do not contain any additional satellites with respect to those reported in single crystals,<sup>5</sup> showing that no additional defects in the vicinity of the Nd ions occur. Moreover, the satellites, associated with perturbing effects of nonstoichiometric excess  $\text{Y}^{3+}$  ions sub-

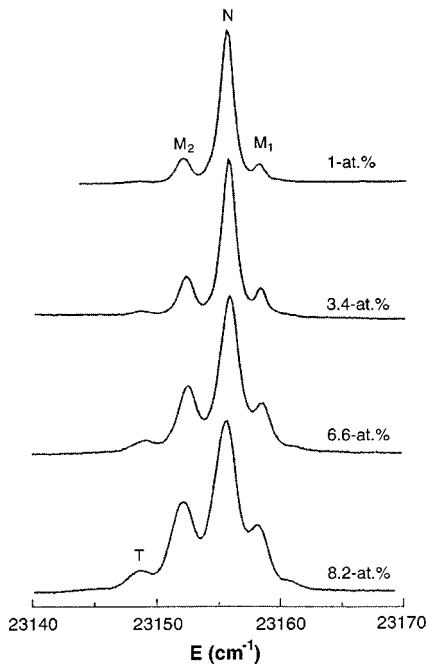


FIG. 1.  ${}^4I_{9/2} \rightarrow {}^2P_{1/2}$  transmission spectra for different concentrations at low temperature.

stituting part of the  $\text{Al}^{3+}$  octahedral  $a$  sites [antisites  $\text{Y}^{3+}(a)$ ] in crystals grown from melt, are almost completely missing in ceramics. In this respect the ceramics are closer to the high-quality crystals grown from flux. This can be explained by the relative low temperature and the solid-state character of the production process. Thus the only major satellites in the transmission spectra of the Nd:YAG ceramics are those connected with crystal-field perturbations inside statistical ensembles of  $\text{Nd}^{3+}$  ions sitting on near-lattice sites. At low Nd concentrations the most important of such ensembles are Nd ion pairs: the satellites corresponding to the first- [nearest-neighbor (NN)] and second- [next-nearest-neighbor (NNN)] order pairs are clearly resolved in most of the optical transitions (satellites  $M_1$ , spectral shift up to 5–6  $\text{cm}^{-1}$ , and  $M_2$ , shift up to 2–3  $\text{cm}^{-1}$ , respectively), as shown in Fig. 1 for the transition  ${}^4I_{9/2}(Z_1) \rightarrow {}^2P_{1/2}$  at various Nd concentrations. In some of the transitions (for instance,  ${}^4I_{9/2} \rightarrow {}^4F_{3/2}$ ) the satellite  $M_2$  is split in two clearly resolved components of equal intensities, while the satellite  $M_1$  is only broadened with a tendency to splitting. The relative intensities of the two satellites with respect to each other or to the line N of the isolated ions (ions that do not participate in the first- or second-order pairs) correspond to the statistics of the random placement of the  $\text{Nd}^{3+}$  ions on the available dodecahedral garnet sites and indicates that the mutual crystal-field perturbations inside of these pairs do not modify the transition probabilities as compared to the ones of the isolated ions. With increasing Nd concentration the relative intensities of the pair lines increase, while the ones of the isolated ions decrease. Moreover, at very high concentrations, new satellites  $T$ , whose relative intensities increase with  $C_{Nd}$  faster than those of the pairs, show up. Most likely these new satellites are connected with triads of  $\text{Nd}^{3+}$  ions on near-lattice sites, the larger spectral shift being consistent

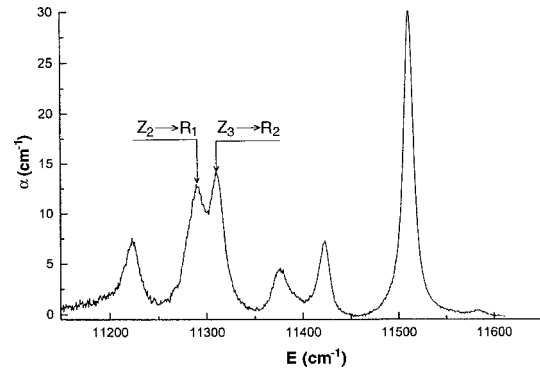


FIG. 2.  ${}^4I_{9/2} \rightarrow {}^4F_{3/2}$  absorption spectrum of 9 at.% Nd:YAG ceramics at room temperature.

with the expected larger mutual crystal-field perturbation inside of these ensembles. Although it was feared that at high  $C_{Nd}$  the large misfit between the ionic radii of  $\text{Nd}^{3+}$  and  $\text{Y}^{3+}$  could force the former ones to aggregate in the vicinity of the surfaces of the ceramic grains, the presence of satellite lines in the optical spectra with intensities corresponding only to the probability of statistical occupation of the dodecahedral sites by the Nd ions shows that no such large-scale aggregation takes place.

With increasing temperature the spectral resolution of the satellite lines is lost; however, the nonresolved pair satellites contribute now to an inhomogeneous line broadening and to an asymmetry of the lines. Although the integral absorption coefficient of the lines scales linearly with  $C_{Nd}$ , the peak absorption coefficients scale sublinearly owing to the concentration-dependent broadening and asymmetrization. The transmission spectra at room temperature enable the selection of optical transitions suitable for diode laser pumping. A very promising such transition could be, for instance, the doubly peaked band centered around 885 nm made up by the hot bands  $Z_2 \rightarrow R_1$  and  $Z_3 \rightarrow R_2$  of the absorption  ${}^4I_{9/2} \rightarrow {}^4F_{3/2}$  (Fig. 2). The cold- or hot-band resonant  ${}^4I_{9/2} \rightarrow {}^4F_{3/2}$  pump was used earlier<sup>10–12</sup> for constructing lasers using 1 at.% Nd:YAG crystals; however, the low pump absorption at this concentration prevents the generation of high laser powers. Our measurements show that the absorption coefficients of the two peaks of the 885-nm band are approximately equal at room temperature and become appreciable at high Nd concentrations: they increase from  $\sim 1.7 \text{ cm}^{-1}$  at 1 at.% Nd to  $\sim 6.5 \text{ cm}^{-1}$  at 4 at.% and  $13\text{--}14 \text{ cm}^{-1}$  at 9 at.% Nd, while the full width at half maximum (FWHM) increases from  $\sim 2.5 \text{ nm}$  at 1 at.% Nd to  $\sim 3.2 \text{ nm}$  at 9 at.% Nd, very suitable for diode laser pumping. Using these hot bands contributes to a considerable reduction of the pump quantum defect as compared to the traditional 808-nm pump into the higher-energy level  ${}^4F_{5/2}$ . This leads to a corresponding improvement of the laser emission characteristics (threshold and slope efficiency) and a drastic reduction of the heat generated in the laser components under pump. This could enhance the potential of concentrated Nd:YAG components for constructing lasers. Hot-band resonant pumping at 1064 nm was used in an attempt to demonstrate laser cooling in a solid (Nd:YAG).<sup>13</sup> The use of

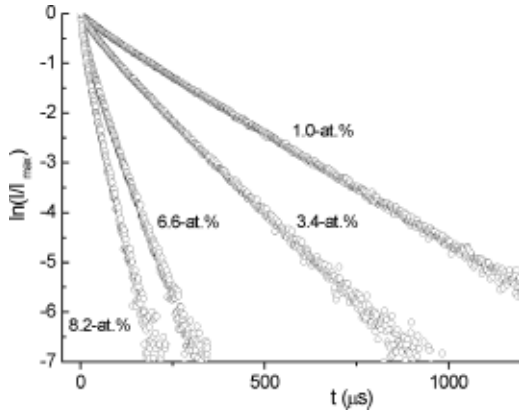


FIG. 3.  ${}^4F_{3/2}$  emission decays for Nd:YAG ceramics of different concentrations at room temperature.

the thermal population of the crystal-field components for hot-band pumping at 885 nm is equivalent to a partial laser cooling that contributes to a reduction of the total heat generated in the pumped material.

The weakly excited emission decay at room temperature is accelerated and shows departures from exponentials with increasing  $C_{Nd}$ , as shown in Fig. 3. The decay can be divided into four successive temporal regions: (i) a very sharp drop that terminates practically within the first two microseconds of the decay and whose extent on the intensity scale increases almost proportionally to  $C_{Nd}$ , (ii) a quasiexponential portion that blurs at high  $C_{Nd}$ , (iii) a nonexponential dependence, and (iv) a new quasiexponential dependence. The border between these regions is not sharp and the transition is gradual. The extent of the regions (ii) and (iii) reduces with increasing  $C_{Nd}$ : region (iv) is not seen in the decay of the diluted samples during 6–8  $e$  foldings of low-noise decay at the low pump intensities used in this experiment. The emission decays of 1 at. % Nd:YAG ceramics and single crystals are similar and can be described by a direct donor-acceptor energy transfer by cross relaxation to intermediate levels, ( ${}^4I_{9/2}$ ,  ${}^4F_{3/2}$ )  $\rightarrow$  ( ${}^4I_{15/2}$ ,  ${}^4I_{15/2}$ ), inside the system of the dopant Nd ions. This modifies the decay to

$$I(t) = I_0 \exp(-t/\tau_D) \exp[-P(t)], \quad (1)$$

where  $\tau_D$  is the lifetime of the emission at very low concentrations, when the energy transfer can be neglected, and  $P(t)$  is the acceptor-ensemble-averaged energy transfer function. In the case of a discrete and random placement of the Nd ions at the available lattice sites,<sup>14,15</sup>

$$P(t) = -\sum \ln[1 - C_A + C_A \exp(-W_i t)], \quad (2)$$

where  $C_A$  is the relative concentration of acceptors and  $W_i$  is the transfer rate to the acceptor placed at the  $i$ th lattice site with respect to the donor. For Nd:YAG under low pumping intensity  $C_A$  is practically equal at any time to the relative concentration of Nd. The fit of Eq. (1) with the transfer function (2) to the experimental data indicates that the ion-ion

interaction responsible for the energy transfer includes contributions from superexchange and dipole-dipole coupling,  $W_i = W_i^{ex} + W_i^{d-d}$  with  $W_i^{ex} = \tau_D^{-1} \exp[2R_0 L^{-1}(1 - R_i/R_0)]$  and  $W_i^{d-d} = C_{DA}/R_i^6$ , where  $L$  is the effective Bohr radius,  $R_0$  is the penetration depth of the superexchange interaction, and  $C_{DA}$  is the energy transfer microparameter of the dipole-dipole interaction.<sup>16,17</sup> A good fit of the decay for 1 at. % Nd:YAG ceramics over six  $e$  foldings is obtained with the parameters determined<sup>18</sup> for single crystals:  $\tau_D = 260 \mu\text{s}$ ,  $L = 0.54 \text{ \AA}$ ,  $R_0 = 5.43 \text{ \AA}$ , and  $C_{DA} \sim 1.8 \times 10^{-40} \text{ cm}^6 \text{ s}^{-1}$ . These energy transfer microparameters explain the unusual form of decay: the very fast initial drop is caused by the very high transfer rate dominated by superexchange inside of the first- (NN) order pairs, while for all the other pairs the transfer is dominated by the dipole-dipole coupling. The quasiexponential portion (ii) can be explained by the linear expansion of the transfer function (2) for low  $C_{DA}$  and  $(W_i t)$  values, i.e.,  $P(t) \sim C_A C_{DA} \sum (W_i t)$ , with the sum excluding the NN sites. For low  $C_{Nd}$  at long times the transfer function  $P(t)$  can be approximated by the function calculated in the approximation of continuous and uniform ion distribution,<sup>16,17</sup> i.e., by  $\gamma t^{-1/2}$  in the case of dipolar coupling, as indeed observed for 1 at. % Nd at times longer than 100  $\mu\text{s}$ . The broadening of the  $M_1$  satellite can be connected with the superexchange interaction inside the NN pairs, while the splitting of satellite  $M_2$  is connected with two possible configurations of the intervening ions for the NNN pairs.

With increasing Nd concentration the extent of the fast initial drop increases, the portion (ii) is blurred, and the  $t^{-1/2}$  dependence of portion (iii) becomes less evident although the decay remains non-exponential, while the quasilinear portion (iv) becomes evident at times progressively shorter. The blurring of portion (ii) is caused by the invalidity of the linear approximation for  $P(t)$  at large  $C_{Nd}$ , while the alteration of the  $t^{-1/2}$  dependence of portion (iii) and the existence of portion (iv) reflect the onset of more and more efficient energy migration processes. It was found that for large Nd concentrations the emission decay can well be described by considering together with the decay terms in Eq. (1) the effect of an additional term  $\exp(-\bar{W}t)$ , where  $\bar{W}$  is an ensemble-averaged migration-assisted energy transfer rate assuming a hopping migration mechanism governed by dipole-dipole interaction,<sup>19</sup>

$$I(t) = I_0 \exp(-t/\tau_D) \exp[-P(t)] \exp(-\bar{W}t), \quad (3)$$

i.e., over the entire decay.

The emission decays for Nd:YAG ceramics in the investigated  $C_{Nd}$  range can be fitted with Eq. (3) by using the intrinsic lifetime  $\tau_D$  and the transfer parameters  $L$ ,  $R_0$ , and  $C_{DA}$  determined from studies on diluted single crystals and assuming that the migration-assisted transfer rate depends quadratically on the Nd concentration,  $\bar{W} = \bar{W}_0 C_{Nd}^2$ , with  $C_{Nd}$  expressed in at. % and  $\bar{W} = 240 \text{ s}^{-1} (\text{at. \%})^{-2} \pm 10\%$ . The error margin is high enough to accommodate additional effects at very high  $C_{Nd}$ , such as a possible modification of the garnet lattice parameter, which cannot be evaluated at the present time.

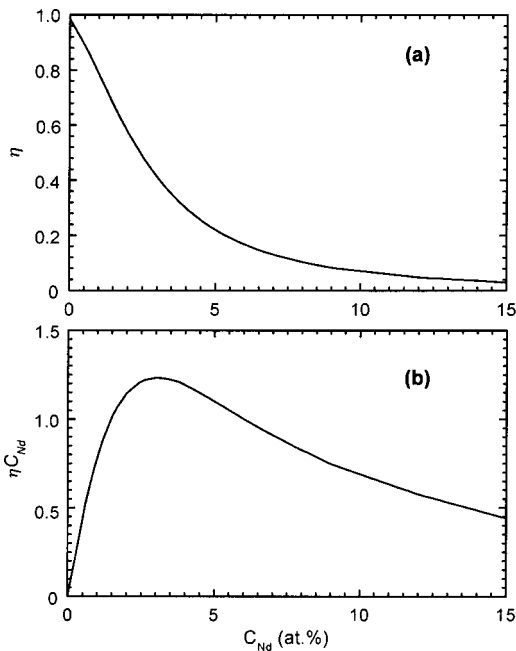


FIG. 4. Calculated concentration dependence of (a) the emission quantum efficiency  $\eta$  and (b) the  $\eta C_{Nd}$  parameter.

The decay law (3) was used to estimate the emission quantum efficiency  $\eta$  in the presence of energy transfer. Its  $C_{Nd}$  dependence is given in Fig. 4(a). The quantum efficiency decreases with increasing  $C_{Nd}$  and all the excitation lost nonradiatively by cross relaxation is transformed into heat. This limits the possibilities of using concentrated Nd:YAG components in laser emission regimes, implying the storage of excitation energy (the  $Q$ -switched regime). However, these materials show good prospect to be used in continuous-wave regimes, where the effect of the reduction of  $\eta$  with increasing  $C_{Nd}$  on the threshold can be compensated by an enhanced absorption of the pump radiation. Although this absorption depends also on the length of the active component, the product  $\eta C_{Nd}$  can be considered as a figure of merit for the expected laser performances at high  $C_{Nd}$ . As shown in Fig. 4(b), this figure of merit is larger than for 1 at. % Nd up to concentrations of 8 at. % Nd and shows a maximum, by about 55% larger than for 1 at. % Nd, in the

region of 3 at. % Nd. This indicates the good prospects of concentrated Nd:YAG components for constructing lasers. Combined with hot-band resonant pumping reducing the generation of heat, these materials could enable the scaling of Nd:YAG lasers to very high powers.

#### IV. CONCLUSION

High-resolution spectroscopy of concentrated (up to 9 at. %) Nd:YAG ceramics indicates that the  $Nd^{3+}$  ions reside on the dodecahedral sites of  $D_2$  symmetry without any major large-scale deformation with respect to the situation encountered in single crystals. These materials do not show spectral satellites to testify the presence of nonstoichiometric  $Y^{3+}$  antisites, characteristic of melt-grown crystals, and from a spectroscopic point of view they approach the compositional and structural perfection of flux-grown crystals. The only obvious clustering effects in these materials originate from the statistical placement of the Nd ions on the available lattice sites. In low-concentrated samples the most probable cluster ensembles are pairs of Nd ions in NN and NNN positions, while the most concentrated samples show also the presence of triads of Nd ions on near-lattice sites. The room-temperature transmission spectra show that at high  $C_{Nd}$  in YAG a very suitable transition for pumping is the broadband centered at 885 nm made up of the hot-band transitions  $Z_2 \rightarrow R_1$  and  $Z_3 \rightarrow R_2$  of the  ${}^4I_{9/2} \rightarrow {}^4F_{3/2}$  absorption: this allows a considerable reduction of the quantum defect and thus of the heat generation. The emission decays of the 1 at. % Nd:YAG ceramics and single crystals are similar. In the concentrated ceramic samples the decay can be described by considering the direct donor-acceptor energy transfer by cross relaxation to intermediate levels inside the system of dopant Nd ions with the parameters determined previously for diluted crystals and by a migration-assisted term whose ensemble-averaged rate scales with  $C_{Nd}^2$ . The figure of merit  $\eta C_{Nd}$  calculated with these parameters has values larger than the one for 1 at. % Nd for concentrations up to 8 at. %, with a maximum at about 3 at. %. This indicates that high-concentrated Nd:YAG components can be used to construct efficient continuous-wave Nd:YAG lasers. Together with pumping into the hot band at 885 nm, these materials show prospects for scaling Nd:YAG lasers to very high powers.

- <sup>1</sup>Y. Zhou, *J. Cryst. Growth* **78**, 31 (1986).  
<sup>2</sup>P. Gavrilovic *et al.*, *Appl. Phys. Lett.* **60**, 1652 (1992).  
<sup>3</sup>D. Pelenc *et al.*, *J. Phys. IV* **1**, 311 (1991).  
<sup>4</sup>A. Ikesue *et al.*, *J. Am. Ceram. Soc.* **78**, 1033 (1995).  
<sup>5</sup>V. Lupei *et al.*, *Phys. Rev. B* **51**, 8 (1995).  
<sup>6</sup>M. Sekita *et al.*, *J. Appl. Phys.* **67**, 453 (1990).  
<sup>7</sup>G. W. Burdick *et al.*, *Phys. Rev. B* **50**, 16 309 (1994).  
<sup>8</sup>M. Klintonberg *et al.*, *Phys. Rev. B* **55**, 10 369 (1997).  
<sup>9</sup>G. W. Burdick *et al.*, *Phys. Rev. B* **59**, R7789 (1999).  
<sup>10</sup>M. Ross, *Proc. IEEE* **56**, 196 (1968).  
<sup>11</sup>L. J. Rosenkrantz, *J. Appl. Phys.* **43**, 4603 (1972).  
<sup>12</sup>R. Lavi and S. Jackel, *Appl. Opt.* **39**, 3093 (2000).  
<sup>13</sup>T. Kushida and S. Geusic, *Phys. Rev. Lett.* **21**, 1172 (1968).  
<sup>14</sup>S. I. Golubov and Yu. V. Konobeev, *Fiz. Tverd. Tela (Leningrad)* **13**, 3185 (1971) [*Sov. Phys. Solid State* **13**, 2679 (1972)].  
<sup>15</sup>V. P. Sakun, *Fiz. Tverd. Tela (Leningrad)* **14**, 2199 (1972) [*Sov. Phys. Solid State* **14**, 1906 (1973)].  
<sup>16</sup>T. Forster, *Ann. Phys. (N.Y.)* **2**, 55 (1958).  
<sup>17</sup>D. L. Dexter, *J. Chem. Phys.* **21**, 863 (1953).  
<sup>18</sup>V. Lupei and A. Lupei, *Phys. Rev. B* **61**, 8087 (2000).  
<sup>19</sup>A. I. Burshtein, *Zh. Eksp. Teor. Fiz.* **62**, 1695 (1972) [*Sov. Phys. JETP* **35**, 882 (1972)].